Theory and simulation of the electrical double layer

D. Boda[1] and D. Henderson

Department of Chemistry and Biochemistry, Brigham Young University,
Provo UT 84602-5700, USA
email: doug@huey.byu.edu

First we give a review of previous theoretical and simulation studies of the electrochemical double layer and then discuss our recent simulations and the anomalous results that we have found at low temperatures, which are seen in experiment but are not predicted by any existing theories. Finally, we outline our future plans.

1. INTRODUCTION; GOUY-CHAPMAN THEORY

The study of the electrochemical double layer (DL) is of interest in aiding in our understanding of electrochemical processes, such as corrosion, at surfaces.

Most experimental results are interpreted in terms of the Gouy-Chapman (GC) theory[1,2]. The GC theory is based on what is called the *primitive model* (PM). In the PM the molecular structure of the solvent, usually water, is ignored. The solvent is represented by a dielectric medium of dielectric constant ε. In the PM the ions are represented by charged hard spheres. A further approximation is the restricted primitive model (RPM), where the ions are all considered to have equal diameter, σ. The GC theory goes one step further and considers the ions to be point charges. The neglect of the molecular nature of the solvent is the more severe approximation. Considering the ions to be point ions is not so bad and a correction called the *Stern layer* can be made. We will discuss the Stern layer shortly.

The GC theory results from the combination of Poisson's equation,

$$\nabla^2 \varphi(x) = -\frac{4\pi}{\varepsilon} q(x) \tag{1}$$

[1] Permanent address: Department of Physical Chemistry, University of Veszprém, H-8201 Veszprém, PO Box 158, Hungary, email: boda@almos.vein.hu

with the Boltzmann approximation,

$$q(x) = \begin{cases} 0 & , \; x < \sigma/2 \\ \sum_i q_i n_i \exp[-\beta q_i \varphi(x)] & , \; x > \sigma/2, \end{cases} \qquad (2)$$

where $\varphi(x)$ is the electrostatic potential and $q(x)$ is the total charge profile, q_i is the charge and n_i is the density (number of ions/volume) of an ion of species i, and $\beta = 1/kT$, where k is the Boltzmann constant and T is the temperature. The parameter x is the distance from the electrode. Obviously, point ions can go right up to the surface, which we assume to be hard. Since the wall is charged, this would lead to difficulties. However, we can prevent this problem by not allowing the ions to get closer than $\sigma/2$ to the wall. What we are doing is taking the ion size into account in the wall-ion interactions but neglecting it for the ion-ion interactions.

The layer of thickness $\sigma/2$ that is devoid of ions is called the Stern layer (or Helmholtz layer, or inner layer, or compact layer). It need not be regarded just as the distance between the ion center of a contact ion and the surface. The Stern layer can be considered as a solvation layer of solvent molecules at the electrode. There is no reason why the thickness of the Stern layer should be $\sigma/2$ or that the dielectric in the Stern layer should have the same value as in the bulk. Thus, we can call d the thickness of the Stern layer and ε^* the value of the dielectric constant in the Stern layer. In principle, d and ε^* can vary with electrode charge. This is often done but it is a little too empirical for this article.

We must have electric neutrality in the bulk,

$$\sum_i q_i n_i = 0 \qquad (3)$$

Furthermore, the charge per unit area in the DL must be equal in magnitude, but opposite in sign, to that on the electrode. Thus

$$\sum_i q_i n_i \int_d^\infty g_i(x)dx = -\frac{E}{4\pi} = -Q \qquad (4)$$

The quantities Q and E are the electrode charge and the field at the electrode. They are related by Gauss' law. The quantity $g_i(x)$ is the distribution function of ions of species i. The density and charge profile of the ions of species i are

$$n_i(x) = n_i q_i(x) \qquad (5)$$

and

$$q_i(x) = n_i q_i g_i(x) \qquad (6)$$

In the GC theory,

$$g_i(x) = \exp[-\beta q_i \varphi(x)] \qquad (7)$$

The Boltzmann relation is not valid in other theories and in simulations.
The potential profile is given by

$$\varphi(x) = -\frac{4\pi}{\varepsilon} \sum_i n_i q_i \int_x^\infty (t-x) g_i(t) dt \qquad (8)$$

It is easy to verify that $\varphi(x)$ satisfies Poisson's equation. From Eq. 8, it is seen
that the potential across the DL is

$$V = \varphi(0) = \varphi(\sigma/2) + \frac{E\sigma}{2\varepsilon} \qquad (9)$$

Equation 4 was used to obtain Eq. 9. Sometimes in simulations or in a theory,
the ability to obtain

$$V - \varphi(\sigma/2) = \frac{E\sigma}{2\varepsilon} \qquad (10)$$

is used as a test of the accuracy of theory. Any theory or simulation that satis-
fies microscopic charge neutrality, Eq. 4, will satisfy Eq. 10 automatically.
A few moments of examination of Eq. 4 shows this. Thus, Eq. 10 is not a real
test, at least for a simulation where charge neutrality is built in from the start.
The right hand side of Eq. 9 may be called the Stern layer potential. The poten-
tial $\varphi(\sigma/2)$ is often called the diffuse layer potential. If a variable thickness and
dielectric constant is used for the Stern layer, the Stern layer potential would be
Ed/ε^*.

The GC equations can be solved analytically to yield $\varphi(x)$, the $g_i(x)$, and V.
For example, for a symmetric salt in the GC theory

$$V = \frac{E\sigma}{2\varepsilon} + \frac{2}{\beta q} \sinh^{-1} \frac{b}{2} \qquad (11)$$

where $b = \beta q E/\varepsilon \kappa$, $\kappa^2 = 4\pi \beta q^2 \rho/\varepsilon$ and $\rho = \sum_i n_i$ is the total density. In ob-
taining Eq. 11 we have assumed that the ions have equal charge. Thus, $q = |q_i|$.
It is of interest to linearize Eq. 11. Thus, at small electrode charge the GC the-
ory gives

$$V = \frac{E\sigma}{2\varepsilon} + \frac{E}{\varepsilon \kappa} \qquad (12)$$

2. SOME RESULTS FOR THE PRIMITIVE MODEL

In Figures 1 and 2, $\varphi(\sigma/2)$ and $g_i(x)$, obtained from the GC theory, are compared with the computer simulations of Torrie and Valleau [3] for a mono-valent salt. The GC theory is based on point ions whereas the simulations are for ions with $\sigma = 4.25$ Å. The agreement is fairly good and certainly better than what one might expect, although it deteriorates somewhat as the electrode charge increases. This indicates that for monovalent salts, the size of the ions is not a major effect. Of course, both the GC theory and the simulations neglect the molecular nature of the solvent so the comparison in Figures 1 and 2 says nothing about the effect of the solvent molecules.

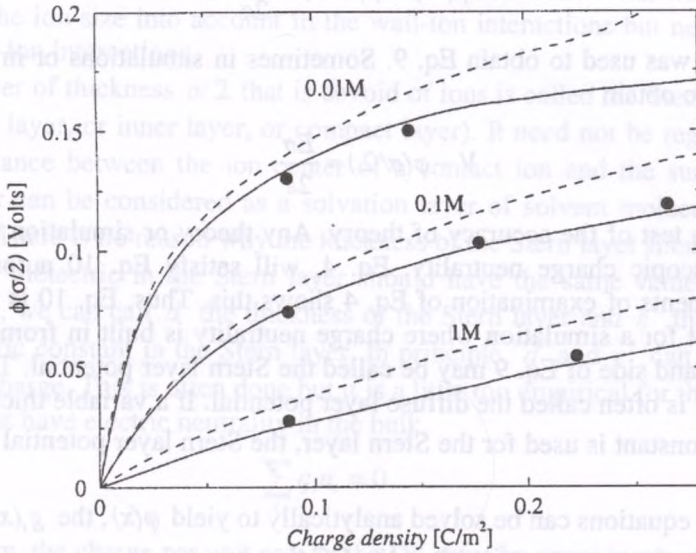The GC theory works less well for higher valence salts.

Figure 1. Diffuse layer potential, $\psi(\sigma/2)$, for a monovalent aqueous electrolyte at 0.01, 0.1, and 1 molar concentrations. The circles give the simulation results of Torrie and Valleau [3]. The dashed and solid curves give the GC and HNC results, respectively

In Figures 3 and 4, the GC theory is compared with the simulations of Torrie and Valleau [4] for 1:2 aqueous electrolytes. When the monovalent ions are the ions attracted to the electrode (2:1 case), the results are much like the results in Figures 1 and 2. However, when the divalent ions (1:2 case) are the ions at-tracted to the electrode, the agreement is much poorer.
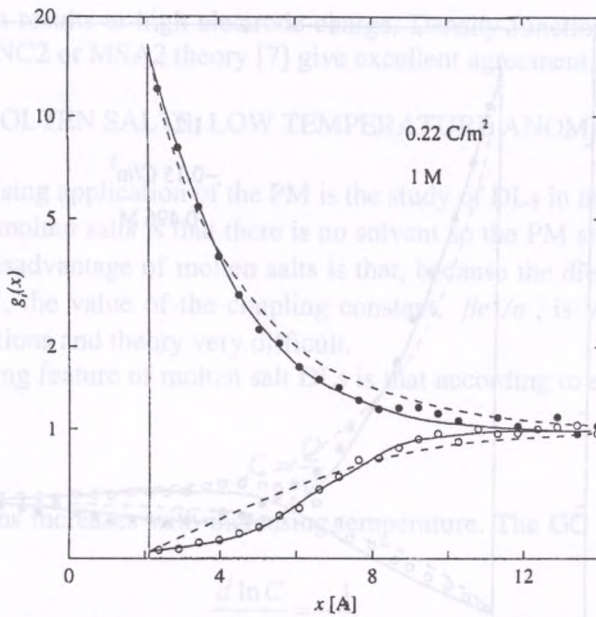
Figure 2. Normalized density profiles, $g_i(x) = n_i(x)/n_i(\infty)$, for a 1 molar monovalent aqueous electrolyte. The circles and curves have the same meaning as in Figure 1
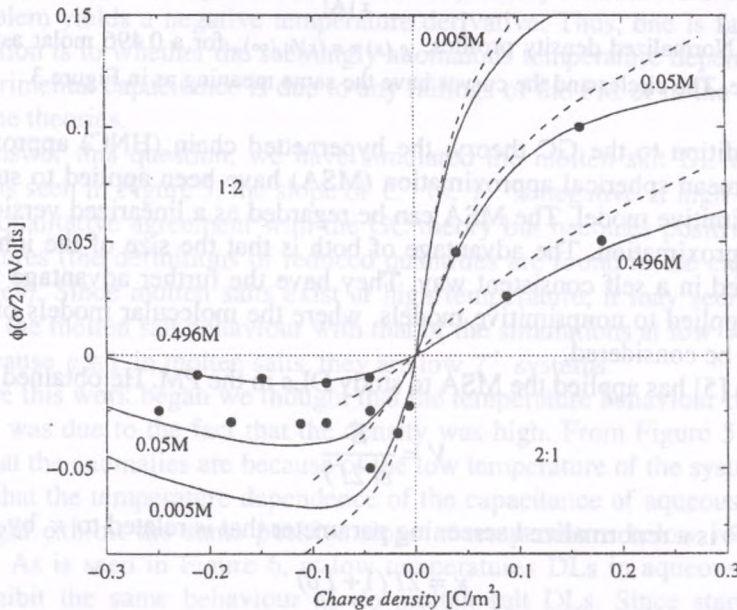

Figure 3. Diffuse layer potential, $\psi(\sigma/2)$, for an asymmetric aqueous electrolyte at 0.005, 0.05, and 0.496 molar concentrations. The circles give the simulation results of Torrie and Valleau [4]. The curves have the same meaning as in Figure 1
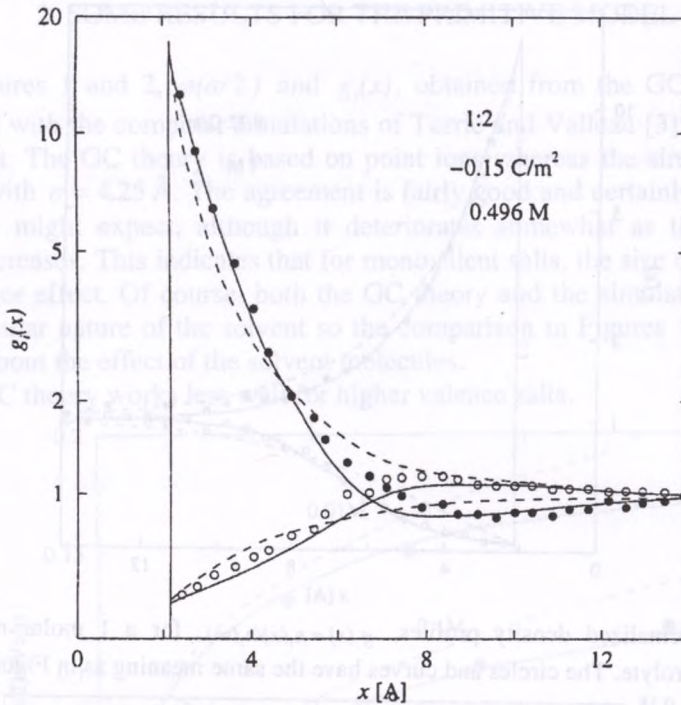
Figure 4. Normalized density profiles, $g_i(x) = n_i(x)/n_i(\infty)$, for a 0.496 molar asymmetric electrolyte. The circles and the curves have the same meaning as in Figure 3

In addition to the GC theory, the hypernetted chain (HNC) approximation and the mean spherical approximation (MSA) have been applied to study DLs in the primitive model. The MSA can be regarded as a linearized version of the HNC approximation. The advantage of both is that the size of the ions can be considered in a self consistent way. They have the further advantage that they can be applied to nonprimitive models, where the molecular models of the solvent can be considered.

Blum [5] has applied the MSA to study DLs in the PM. He obtained

$$V = \frac{E}{\varepsilon(2\Gamma)} \tag{13}$$

where Γ is a renormalized screening parameter that is related to κ by

$$\kappa = 2\Gamma(1 + \Gamma\sigma) \tag{14}$$

Expansion of Eq. 13 in powers of κ leads to Eq. 12 as one would hope.

As is seen in Figures 1-4, the HNC results are in better agreement with the simulation results than are the GC results. The HNC results fail to agree with

the simulation results at high electrode charge. Density functional (DF) theory [6] and the HNC2 or MSA2 theory [7] give excellent agreement.

3. MOLTEN SALTS; LOW TEMPERATURE ANOMALIES

One promising application of the PM is the study of DLs in molten salts. The advantage of molten salts is that there is no solvent so the PM should be a good model. The disadvantage of molten salts is that, because the dielectric constant is 1 or near 1, the value of the coupling constant, $\beta e^2/\sigma$, is very large. This makes simulations and theory very difficult.

One puzzling feature of molten salt DLs is that according to experiments the capacitance

$$C = \frac{Q}{V} \tag{15}$$

in such systems increases with increasing temperature. The GC theory predicts that

$$\frac{d\ln C}{d\ln T} = -\frac{1}{2} \tag{16}$$

which has the opposite sign. Furthermore, every theory that has been applied to this problem yields a negative temperature derivative. Thus, one is faced with the question is to whether the seemingly anomalous temperature dependence of the experimental capacitance is due to any failings of the PM or to the deficiencies of the theories.

To answer this question, we have simulated the molten salt DL using the PM. As is seen in Figure 5, the slope of C^* vs. T^* is negative at high temperatures in qualitative agreement with the GC theory but becomes positive at low temperatures (the definitions of reduced quantities are found in the captions of the figures). Since molten salts exist at high temperature, it may seem odd to compare the molten salt behaviour with that of the simulations at low T^*. However, because $\varepsilon \cong 1$ in molten salts, they are low T^* systems.

Before this work began we thought that the temperature behaviour of molten salt DLs was due to the fact that the density was high. From Figure 5 it is apparent that the anomalies are because of the low temperature of the system. This suggest that the temperature dependence of the capacitance of aqueous electrolytes might exhibit the same positive slope at temperatures below room temperature. As is seen in Figure 6, at low temperatures DLs in aqueous electrolytes exhibit the same behaviour as do molten salt DLs. Since starting this study, W. Schmickler has drawn our attention to the study of Hamelin et al. [8] who found that the DL capacitance of $HClO_4 \cdot 5.5H_2O$ at temperatures between 200 K and 300 K decreases with decreasing temperature.
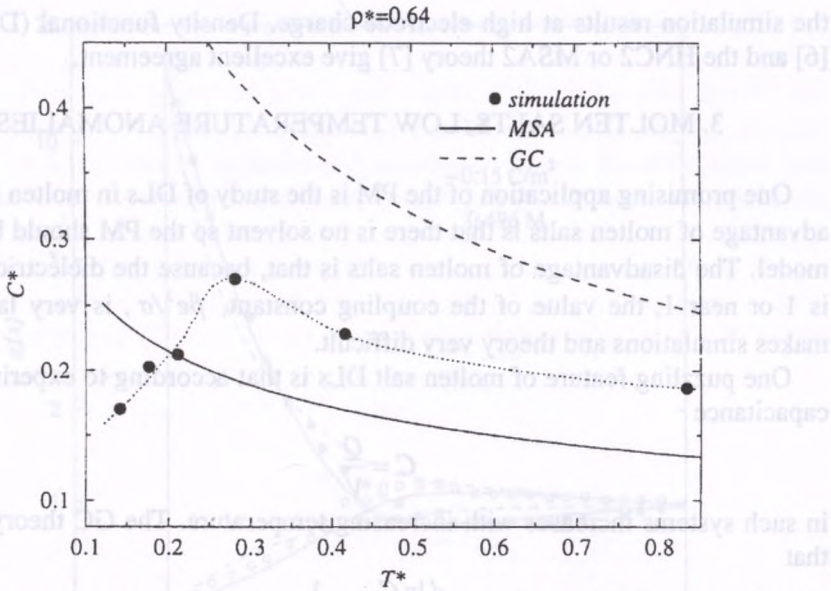
Figure 5. Reduced capacitance, $C^* = Q\sigma/V$, for a model salt double layer as a function of the reduced temperature, $T^* = \sigma kT/e^2$. The reduced density is typical of a liquid: $\rho^* = \rho\sigma^3 = 0.64$. The dotted line is to guide the eye
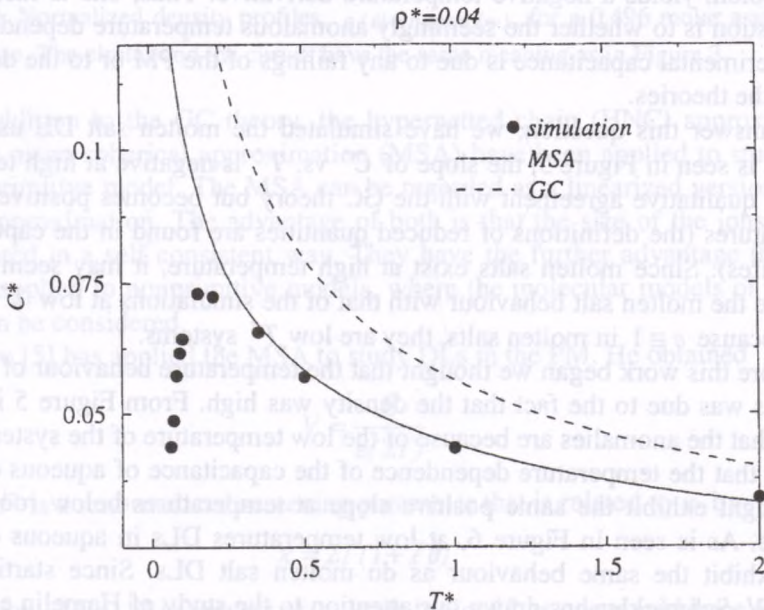

Figure 6. Reduced capacitance, $C^* = Q\sigma/V$, for the double layer in the PM as a function of the reduced temperature, $T^* = \sigma kT/e^2$, near the critical temperature. The reduced density is low: $\rho^* = \rho\sigma^3 = 0.04$

Regrettably, the MSA cannot account for the positive slope of C^* vs. T^* that we have seen in our simulations. The HNC approximation has not been tried in this application but in view of its relation to the MSA there is no reason to expect it to be successful. Disappointingly, the DF theory fails also. The HNC2 and MSA2 approaches have not been used yet for this problem.
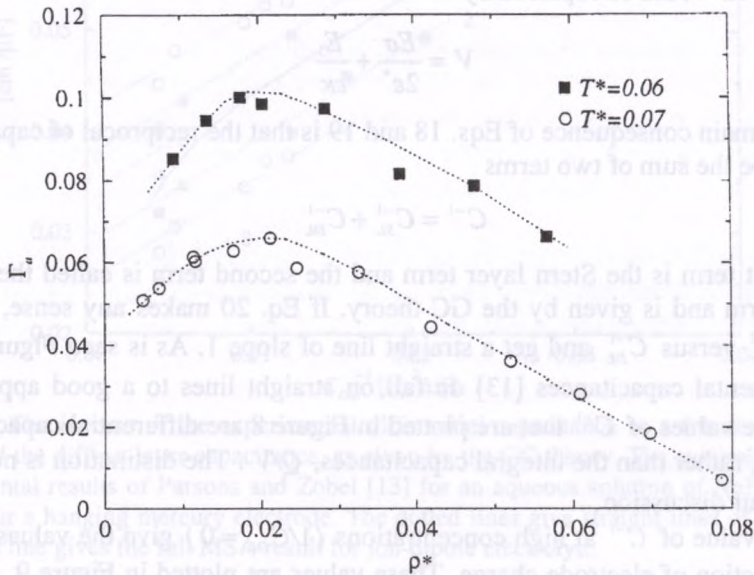

Figure 7. The adsorption isotherms of the PM as a function of the reduced density at two temperatures close to the critical temperature. The electrode charge density is $Q\sigma^2/e = 0.03$. The dotted lines are to guide the eye

According to simulations, there is a critical point in electrolytes at $T^* \sim 0.05$ and $\rho^* \sim 0.025$ [9, 10, 11]. The value of T^* is better established than the value of ρ^*. In any case, Henderson et al. [12] have presented qualitative arguments that the adsorption isotherm,

$$\Gamma_a = \sum_i n_i \int [g_i(x) - 1] dx \qquad (17)$$

would be large in the near vicinity of the critical point. As is seen in Figure 7, this is supported by our simulation studies.

4. NONPRIMITIVE MODELS

As we have mentioned, the simplest method for taking the solvent into account is to give the Stern layer a different thickness or more importantly a low dielectric constant. This latter semiempirical change mimics the presumed fact

that the solvent molecules are oriented near the electrode. Using the latter modification, Eq. 11 would be replaced by

$$V = \frac{E\sigma}{2\varepsilon^*} + \frac{2}{\beta q}\sinh^{-1}\frac{b}{2} \tag{18}$$

and Eq. 12 would be replaced by

$$V = \frac{E\sigma}{2\varepsilon^*} + \frac{E}{\varepsilon\kappa} \tag{19}$$

The main consequence of Eqs. 18 and 19 is that the reciprocal of capacitance would be the sum of two terms

$$C^{-1} = C_{SL}^{-1} + C_{DL}^{-1} \tag{20}$$

The first term is the Stern layer term and the second term is called the diffuse layer term and is given by the GC theory. If Eq. 20 makes any sense, we can plot C^{-1} versus C_{DL}^{-1} and get a straight line of slope 1. As is seen Figure 8, the experimental capacitances [13] do fall on straight lines to a good approximation. The values of C^{-1} that are plotted in Figure 8 are differential capacitances, dQ/dV, rather than the integral capacitances, Q/V. The distinction is not material to our discussion.

The value of C^{-1} at high concentrations $(1/C_{DL}=0)$ give the values of C_{SL}^{-1} as a function of electrode charge. These values are plotted in Figure 9. Clearly, if Eq. 18 were to be used, ε^* would have to be a function of electrode charge. We will not do this. Our attention will be directed to the zero charge case.

The next step in sophistication would be to represent the solvent by hard spheres and to retain the dielectric background. The hard sphere solvent would account for the excluded volume effect. This has been done by Henderson and Lozada-Cassou [14] and by Tang et al. [15]. The latter authors called this the *solvent primitive* (SP) model. Tang et al. have made simulations for this model. At zero electrode charge, the MSA gives Eq. 12 or 19.

The main result for the SP model is to cause strong oscillations in the density profiles. Since they affect the positive and negative ions in much the same manner, the potential and capacitance are not so strongly affected. Even so if the profiles differ appreciably from the GC predictions, the microscopic picture is quite different. Oscillations in profiles have been seen in experimental determinations of the force between macroscopic bodies immersed in electrolytes [16]. Since electrochemical reactions are, presumably, affected by the microscopic situations, many ideas in electrochemistry should be reexamined.
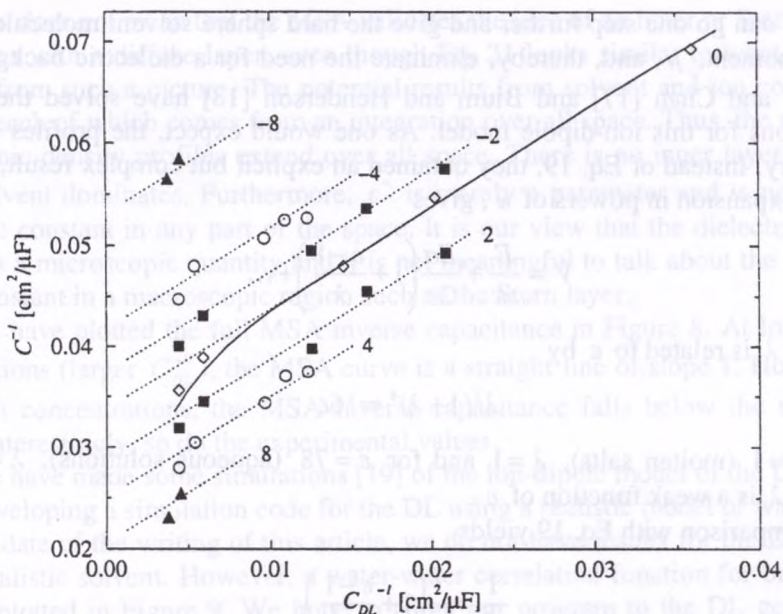
Figure 8. The inverse of the experimental differential capacitance as a function of the inverse of the diffuse layer capacitance, as given by the GC theory. The symbols are the experimental results of Parsons and Zobel [13] for an aqueous solution of NaH$_2$PO$_4$ at 25 ^{0}C near a hanging mercury electrode. The dotted lines give straight lines of slope 1. The solid line gives the full MSA result for ion-dipole electrolyte
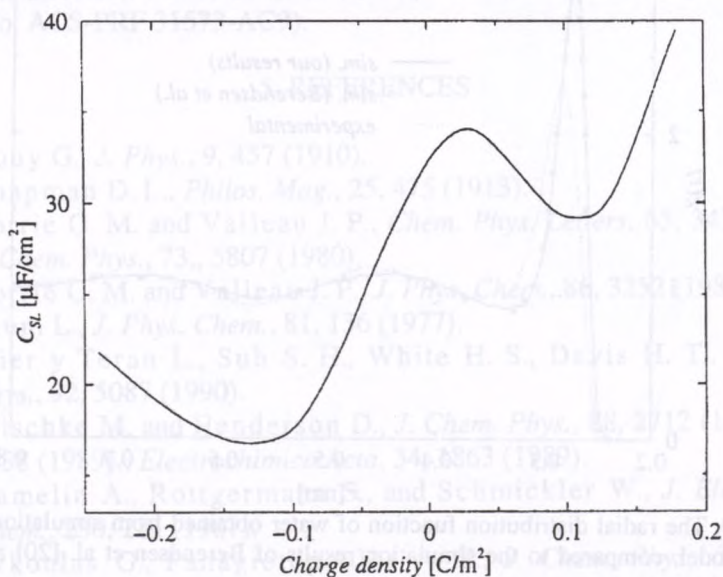

Figure 9. Plot of the intercepts of the straight lines in Figure 8 with the $C_{DL}^{-1} = 0$ axis as a function of the electrode charge density

We can go one step further and give the hard sphere solvent molecules a dipole moment, μ, and, thereby, eliminate the need for a dielectric background. Carnie and Chan [17] and Blum and Henderson [18] have solved the MSA equations for this ion-dipole model. As one would expect, the profiles are oscillatory. Instead of Eq. 19, they obtained an explicit but complex result, which upon expansion in powers of κ, gives

$$V = \frac{E}{\varepsilon\kappa} + \frac{E\sigma}{2\varepsilon}\left(1 + \frac{\varepsilon-1}{\lambda}\right) + \dots \tag{21}$$

where λ is related to ε by

$$\lambda^2(1+\lambda)^4 = 16\varepsilon \tag{22}$$

For $\varepsilon = 1$ (molten salts), $\lambda = 1$ and for $\varepsilon = 78$ (aqueous solutions), $\lambda = 2.65$. Thus, λ is a weak function of ε.

Comparison with Eq. 19 yields

$$\frac{1}{\varepsilon^*} = \frac{1}{\varepsilon}\left(1 + \frac{\varepsilon-1}{\lambda}\right) \tag{23}$$

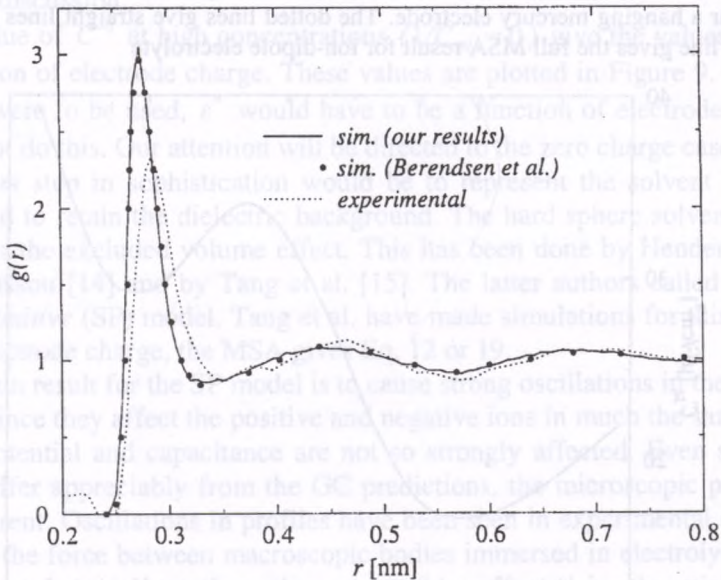which gives a value for ε^* that is similar to that used in fits to experiment.

Figure 10. The radial distribution function of water obtained from simulation using the SPC/E model, compared to the simulation results of Berendsen et al. [20] and the experimental curve

This does not mean that the MSA validates the idea of an inner or Stern layer in series with a diffuse layer, even though Eq. 21 looks similar to what would result from such a picture. The potential results from solvent and ion contributions, each of which comes from an integration over all space. Thus, the solvent and ionic density profiles extend over all space. There is no inner layer where the solvent dominates. Furthermore, ε^* is merely a parameter and is not a dielectric constant in any part of the space. It is our view that the dielectric constant is a microscopic quantity and it is not meaningful to talk about the dielectric constant in a macroscopic region such as the Stern layer.

We have plotted the full MSA inverse capacitance in Figure 8. At low concentrations (larger C_{DL}^{-1}), the MSA curve is a straight line of slope 1. However, at high concentrations, the MSA inverse capacitance falls below the straight line. Interestingly, so do the experimental values.

We have made some simulations [19] of the ion-dipole model of the DL. We are developing a simulation code for the DL using a realistic model of water. As of the date of the writing of this article, we do not have results for the DL with this realistic solvent. However, a water-water correlation function for bulk water is plotted in Figure 9. We hope to adopt our program to the DL geometry and be able to report results in the near future.

5. REFERENCES

[1]   Gouy G., *J. Phys.*, 9, 457 (1910).

[2]   Chapman D. L., *Philos. Mag.*, 25, 475 (1913).

[3]   Torrie G. M. and Valleau J. P., *Chem. Phys. Letters*, 65, 343 (1979).; *J. Chem. Phys.*, 73,, 5807 (1980).

[4]   Torrie G. M. and Valleau J. P., *J. Phys. Chem.*, 86, 3252 (1982).

[5]   Blum L., *J. Phys. Chem.*, 81, 136 (1977).

[6]   Mier y Teran L., Suh S. H., White H. S., Davis H. T., *J. Chem. Phys.*, 92, 5087 (1990).

[7]   Plischke M. and Henderson D., *J. Chem. Phys.*, 88, 2712 (1988).; 90, 5738 (1989).; *Electrochimica Acta*, 34, 1863 (1989).

[8]   Hamelin A., Rottgermann S., and Schmickler W., *J. Electroanal. Chem.*, 230, 281 (1987).

[9]   Orkoulas G., Panagiotopoulos A. Z., *J. Chem. Phys.*, 101, 1452 (1994).

[10] Caillol J. M., Levesque D., and Weis J. J., *J. Chem. Phys.*, 107, 1565
       (1997).
[11] Valleau J. and Torrie G., *J. Chem. Phys.*, 108, 5169 (1998).
[12] Henderson D., Barojas J., and Blum L., *J. Phys. Chem.*, 87, 4544
       (1983).
[13] Parsons R. and Zobel F. G. R., *J. Electroanal. Chem.*, 9, 333 (1965).
[14] Henderson D. and Lozada-Cassou M., *J. Colloid Interface Sci.*, 114,
       180 (1986).
[15] Tang Z., Scriven L. E., and Davis H. T., *J. Chem. Phys.*, 97, 9258
       (1992).
[16] Izraelachvili J., *Intermolecular and Surface Forces*, 2nd Ed., Aca-
       demic Press, London, 1992.
[17] Carnie S. L. and Chan D. Y., *J. Chem Phys.*, 73, 2949 (1980).
[18] Blum L. and Henderson D., *J. Chem. Phys.*, 74, 1902 (1981).
[19] Boda D., Chan K. Y., and Henderson D., *J. Chem. Phys.*, 109, 7362
       (1998).
[20] Berendsen H. J. C., Grigera J. R., Straatsma T. P., *J. Phys. Chem.*,
       91, 6269 (1987).

CURRICULA VITAE
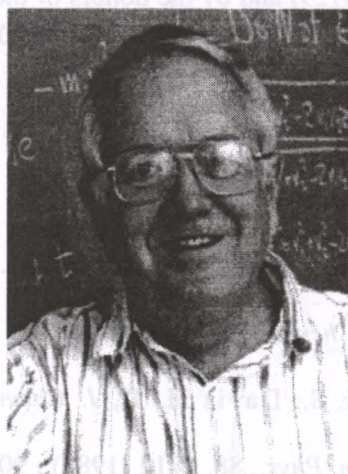
Prof. Douglas Henderson. He was born in Canada in 1934 and graduated in mathematics from the University of British Columbia. He obtained his Ph.D. in physics from the University of Utah under the supervision of Henry Eyring. He has spent twenty years in the IBM Research Division and has been at Brigham Young University since 1995. His main interest is the application of statistical mechanics to liquids and their interfaces. He has published over 350 papers and has written a book *"Statistical Mechanics and Dynamics"* (Wiley 1964 and 1981) with Henry Eyring. He also coedited the eleven – volume *"Treatise on Physical Chemistry"* (Academic Press 1967-1975). He has received several awards for his research, most recently the American Chemical Society Joel Henry Hildebrand Award. He has visited many scientific institutions, including long visits to the CSIRO laboratory in Melbourne, Australia and the Universidad Autonoma Metropolitana in Mexico City. He has been a frequent visitor at the Faculty of Chemistry of MCS University in Lublin.
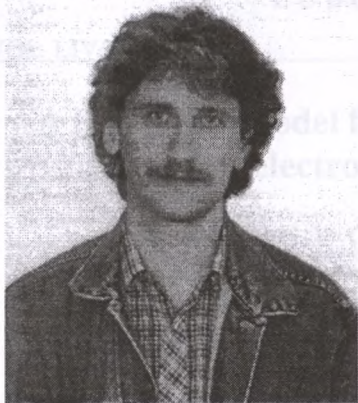
Dr. Dezsö Boda. He was born in 1967 and graduated in physics from the József Attila University in Hungary in 1992. He was a Ph.D. student at the Department of Physical Chemistry in the University of Veszprém, Hungary, under the supervision of Professor János Liszi and Dr. István Szalai for three years. They developed new simulation methods to determine the vapour-liquid equilibrium of pure bulk fluids. After obtaining his Ph.D. in 1996, he went to Hong Kong and worked in the University of Hong Kong with Dr. K. Y. Chan. There he started investigating inhomogeneous systems such as electrochemical double layers. It was also in Hong Kong where he started the collaboration with Professor Douglas Henderson. He has held a position at the Department of Physical Chemistry in the University of Veszprém since 1997. Since the September of 1998, he has been engaged in research in Brigham Young University with Professor Douglas Henderson.